

# DEVELOPING A GENERALIZED FRAMEWORK FOR ASSESSING SAFETY OF HYDROGEN VEHICLES IN TUNNELS

Schroeder, B.B.<sup>1</sup>, Ehrhart, B.D.<sup>1</sup> Brooks, D.M.<sup>1</sup>, Bran Anleu, G.A.<sup>2</sup>, and Blaylock, M.L.<sup>2</sup>

<sup>1</sup> Risk & Reliability Analyses, Sandia National Laboratories, Albuquerque, NM, 87185, USA, [bbschro@sandia.gov](mailto:bbschro@sandia.gov), [bdehrha@sandia.gov](mailto:bdehrha@sandia.gov), [dbrooks@sandia.gov](mailto:dbrooks@sandia.gov)

<sup>2</sup> Thermal/Fluid Science & Engineering, Sandia National Laboratories, Livermore, CA, 94550, USA, [gabrana@sandia.gov](mailto:gabrana@sandia.gov), [mlblayl@sandia.gov](mailto:mlblayl@sandia.gov)

## ABSTRACT

For widespread adoption of hydrogen fuel cell powered vehicles, such vehicles need to be able to provide similar transportation capabilities as their gasoline/diesel powered counterparts. Meeting this requirement in many regions will necessitate access to tunnels. Previous work completed at Sandia National Laboratories provided high-fidelity consequence modeling of hydrogen vehicle tunnel crashes for a specific fire scenario in selected Massachusetts tunnels. To consider additional tunnels, a generalized tunnel safety analysis framework is being developed. This framework aims to be broader than specific fire scenarios in specific tunnels, allowing it to be applied to a range of tunnel geometries, vehicle types, and crash scenarios. Initial steps in the development of the generalized framework are reported within this work. Representative tunnel characteristics are derived based on data for tunnels in the U.S. Tunnel dimensions, shapes, and traffic levels are among the many characteristics reported within the data that can be used to inform crash scenario specification. Various crash scenario parameters are varied using lower-fidelity consequence modeling to quantify the impact on resulting safety hazards for time-dependent releases. These lower-fidelity models consider the unignited dispersion of hydrogen gas, the thermal effects of jet fires, and potential impacts of overpressures. Different sizes/classes of vehicles are considered, as the total amount of hydrogen onboard may greatly affect scenario-specific consequences. The generalized framework will allow safety assessments to be both more agile and consistent when applied to different types of tunnels.

## 1.0 INTRODUCTION

As with any type of vehicle, the safety of alternative fuel vehicles in tunnels must be considered as the adoption of these technologies becomes more widespread. The fire, toxicity, and explosion risks posed by alternative fuel vehicles may differ from those previously presented by gasoline/diesel powered vehicles. Such risks may impact the health of humans within tunnels, but also may cause damage to the tunnel structure. Damaged tunnels can pose both an immediate risk to humans within the tunnels as well as cause long term logistical issues impacting the surrounding community and economy if the damage is significant enough to require temporary tunnel closure. This work focuses upon human safety risks posed by hydrogen (H<sub>2</sub>) powered vehicles in tunnels and the risk posed to the tunnel structure. From this study it is hoped that information generated can help inform authorities when making decisions about allowing alternative fuel vehicles, especially H<sub>2</sub> powered vehicles, to move through their tunnel infrastructure. Decisions like tunnel access have a large impact on the ability for alternative fuel vehicles to gain significant adoption and market share.

Prior work on tunnel safety has largely focused on modeling of consequences from scenarios with high safety concerns. High-fidelity consequence modeling involves 3D computational fluid dynamics (CFD) simulations of the hydrogen flame as well as finite element analysis for heat transfer into the ceiling of the tunnels. Low-fidelity consequence modeling includes lower order, 2D analytical models that calculate the flame length and heat flux for ignited hydrogen releases and overpressure models for cases with delayed ignition. LaFleur et al. 2017 [1] explored tunnel thermal criteria using lower-fidelity modeling, but then applied high-fidelity modeling to analyse a specific hydrogen vehicle crash scenario for specific tunnel geometries for the Massachusetts Department of Transportation. A literature review completed by Sandia National Laboratories [2] reviewed experimental, modeling, and analysis efforts involving the hazards posed by alternative fuel vehicles in tunnels. While a significant body of work in this area was reviewed, that work does not apply more generally because

of its high specificity and fidelity. Recently, a report out of the HyTunnel project [3] outlined their work in assessing the safety of alternative fuel vehicles in parking garages and tunnels. This work discussed its findings from experiments and modeling of thermal and overpressure hazards but focused on specific scenarios. Questions remain regarding this work's findings due to its focus on a pressure vessel technology not currently approved by vehicle regulators.

While high-fidelity consequence modeling has been previously relied upon to inform tunnel safety for a few specific tunnel geometries, this capability is not scalable as large quantities of tunnels are considered. An alternative approach is to utilize lower-order models within a generalized tunnel safety analysis framework. A generalized approach is needed because tunnel owners need access to risk information to make decisions in a timely manner. High fidelity modeling one tunnel at a time will not meet the timing needs of regulators or the resources available for analyses. Lower-order models can provide physics-based estimates at a lower resolution than high-fidelity models, but with the major advantage of order of magnitude reductions in computational costs. To be generalized, the framework needs the flexibility to account for variation in factors impacting its predictions including tunnel height, fuel quantity, leak direction, leak duration, and ventilation. Outputs from the framework then need to inform safety for potential hazards resulting from a vehicle accident within the tunnel.

The work reported herein establishes initial steps in the development of the generalized tunnel safety analysis framework. Tunnel characteristics are parsed from a U.S. tunnel inventory database that can be used to inform the framework's construction. Through understanding common characteristics of U.S. tunnels, the framework will be able to provide safety assessments for most tunnels. Crash scenarios can be parameterized in terms of attributes impacting the resulting safety hazards such as fuel quantity, release orifice size, and fuel type. Lower-order modeling is used to explore the impact of scenario parameters on potential consequences for time-dependent releases including jet fires and overpressure events through parameter studies. Scenario parameters studied include tank orifice size, tank size, tank fill level, as well as different alternative fuel types. A single crash scenario is explored within this work to demonstrate lower-order modeling capabilities, but as the framework's development continues it will be applied to a range of other scenarios of concern for tunnel safety.

## **2.0 METHODOLOGY**

The accident scenario considers an alternative fuel vehicle involved in a severe multivehicle accident, flipping on to its roof and being exposed to a fire from a nearby vehicle. This heat exposure results in the thermally-activated pressure relief device (TPRD) on the vehicle's fuel tank activating, causing a jet of fuel to empty directed straight up towards the tunnel ceiling. The time-dependent decay of the jet release, referred to as blowdown, causes the resulting consequences to also have time-dependent responses. Potential consequences of the jet release considered are immediate ignition resulting in a jet flame or delayed ignition resulting in an unconfined overpressure event. Which of the consequences is likely to occur depends on if the external fire impacts the tank near the TPRD or heats up a different section of the tank. The distance between the release point for the fuel and the ceiling is 3.93 meters; this distance will be used to specify when jet flames impinge on the ceiling. While this scenario is deemed an unlikely event, it can be used to compare to previous high-fidelity modeling results and provide insights into how different fuel types behave in extreme crash scenarios.

The H<sub>2</sub> fuelled light duty vehicle considered has a single 125 L tank containing H<sub>2</sub> at 70 MPa with a 2.25 mm TPRD. While most of this work is focused on H<sub>2</sub> vehicles, compressed natural gas (CNG) and liquified petroleum gas (LPG), also known as autogas, light duty vehicles are also considered as points of comparison. The CNG vehicle considered has a single 60 L tank containing 25 MPa CH<sub>4</sub> and the LPG vehicle has a 50 L tank 80% full of liquid propane. Both the CH<sub>4</sub> and LPG tanks are assumed to have the same 2.25 mm TPRD size as the H<sub>2</sub> tank. The vehicle fuel tank characteristics specified thus far are the baseline specifications that will be altered during parameter studies within Section 3 to assess the impact of varying elements of the specifications.

Hazard assessment for this accident scenario is focused on the tunnel ceiling's structural integrity when exposed to potential thermal consequences, though the modeling approaches could also be applied to directly assess human safety within the tunnel. Hazards considered for the ceiling's structural integrity include the ceiling gas temperature as well as the overpressure it experiences. When experiencing direct flame impingement, it is assumed that the ceiling gas temperature is equal to the flame temperature. When the flame is not impinging on the ceiling it heats the gas touching the ceiling through radiative heat transfer [1]. A ceiling gas temperature criterion will not be enacted in the analyses reported herein, but ceiling gas temperature will be compared to design requirements in future work. It should also be noted that the ceiling gas temperature is different from the ceiling temperature, which will require modeling of heat transfer through the ceiling material to characterize. While not modeling reflections of pressure waves off surfaces in the tunnel, overpressure at distances from the overpressure event are used to make relative estimates of the potential damaging impacts. Overpressure values of 21, 14, and 7 kPa are used as indicators of extreme, major, and medium building damage [4].

## 2.1 Lower-Order Physics Modeling

To make predictions of the physical phenomena potentially occurring during the accident scenario, the Hydrogen Plus Other Alternative Fuels Risk Assessment Models (HyRAM+) software toolkit is utilized. HyRAM+ is a free and open-source software developed at Sandia National Laboratories and downloadable from [5]. HyRAM+ has a graphic user interface, but this work leverages its Python backend capabilities, which are also distributed independently through the Python Package Index (<https://pypi.org/project/hyram/>) or Anaconda's conda-forge (<https://anaconda.org/conda-forge/hyram>). Descriptions of the lower-order physics implementations can be found within the HyRAM+ technical manual [6], but the algorithmic approach for estimating blowdowns and associated consequences is described hereafter.

### Blowdown Modeling

To calculate tank blowdown for gaseous fuels, the stored fuel is specified in terms of composition, temperature, and pressure; the orifice is specified in terms of diameter and discharge coefficient; and the surrounding ambient environment is specified in terms of the composition, temperature, and pressure. An ambient temperature of 300 K is assumed for both the fuel and the surrounding environment throughout all blowdown calculations and an ambient pressure of 101,325 Pa is assumed for the ambient environment. An ambient relative humidity of 50% is assumed for radiative heat flux calculations. A conservative discharge coefficient of 1 is assumed for the orifice and the leak is pointed in the vertical direction. Blowdown calculations provide temporal profiles for mass flow rate, tank pressure, and remaining tank fuel mass. Pressure and mass flow rate information is then passed to jet plume and jet fire calculations. HyRAM+ currently supports steady state predictions for jet plume and jet fire calculations, so to calculate temporal evolving consequences, steady state predictions are made for each blowdown timepoint. Due to the releases being choked flows, only the temporal pressure data is used to specify the follow-on consequence calculations. Near the end of the releases the flows stop being choked and the mass flow rate information from the blowdown calculations is also used to specify the corresponding consequence calculations. The choked flow mass flow rates calculated in consequence models are slight underpredictions compared to those found in the blowdown calculations, resulting in consequence estimates also being slight under predictions.

For comparing consequences to other alternative fuels, the modeling approach described thus far needs to be modified to accommodate propane. Whereas H<sub>2</sub> and CNG are stored as compressed gases, LPG is stored as a pressurized liquid at equilibrium with gas filling the remaining tank volume. Due to this difference in phase, an effective density is used to specify the fuel in the tank and the temporal trace of effective density is passed to the consequence models instead of pressure. Effective density is calculated as the remaining mass divided by the tank volume. A validation assessment was recently performed for consequence calculations of CNG and LPG [7].

## Consequence Models

Steady state jet flame calculations provide visible flame length and positional radiative heat flux predictions using HyRAM+'s built-in capabilities. HyRAM+ calculates jet fires as evolving along a streamline and radially out from the streamline. The streamline is the centerline of the jet, which is generally not straight due to buoyancy, but will be for the scenario considered due to being directed straight up. The temperature at the flame tip is estimated based on the combustion product concentrations at the end of the streamline. Wall effects are not included in HyRAM+, so predicted flame lengths can go beyond the ceiling height in the scenario considered. When the flame length is greater than the ceiling height, it is assumed that the flame stops at the ceiling. When estimating the temperature of gas on touching the ceiling, the flame tip temperature, which is hotter than mid-flame temperatures, is assumed while the flame is impinging, and a radiative flux-based flame temperature is assumed thereafter [1]. Figure 1 shows the jet flame profile calculated using HyRAM+ that corresponds to the conditions predicted for the H<sub>2</sub> fuel tank initial blowdown.

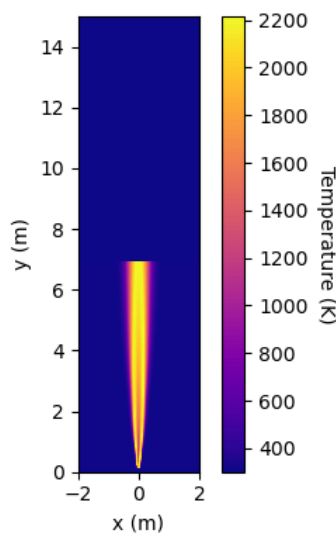


Figure 1. Jet flame simulated by HyRAM+ for initial blowdown response of H<sub>2</sub> fuel tank

To calculate flammable mass and the potentially resulting unconfined overpressure, jet plume calculations and built-in HyRAM+ capabilities are used. Figure 2 shows the jet plume molar concentration profile calculated using HyRAM+ that corresponded to the conditions predicted for the H<sub>2</sub> fuel tank blowdown; the 4% H<sub>2</sub> mole fraction contour is shown due to being the lower flammability limit.

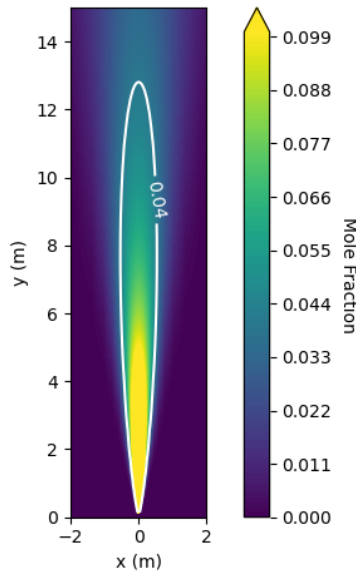


Figure 2. Jet plume simulated by HyRAM+ for first timestep of H<sub>2</sub> fuel tank blowdown

The Baker-Strehlow-Tang unconfined overpressure model with a Mach flame speed of 0.35 is used with a specified blast curve. The blast curves are constructed as scaled peak-overpressures being functionally dependent on scaled-distances. Due to the curves' asymptotes at short scaled-distances, overpressure predictions one meter away from the overpressure event's origin are used as a representative estimate of the overpressure strength. If overpressure is calculated too close to the origin when using blast curves, many scenarios are indistinguishable due to this numerical extrapolation, even when their impact on the surrounding environment can differ significantly. Modeling hydrogen cloud overpressure events in tunnels with an unconfined overpressure model may be an underestimation depending on the volume of the flammable cloud and the tunnel geometry. Appropriate limits for this assumption have yet to be explored within this work.

## 2.2 Federal Highway National Tunnel Inventory

The Federal Highway Administration, a division of the U.S. Department of Transportation (DOT), maintains a National Tunnel Inventory [8]. This inventory is a database comprised of annual data on tunnel characteristics and inspection results for tunnel elements. Reported tunnel characteristics include each tunnel's location, year built, annual average traffic, length, minimum vertical clearance, roadway width, shape, as well as many other attributes. Elements inspected are based on each tunnel's unique elements and include the tunnel liner, roof girders, ceiling slab, ceiling panels, and ventilation system. The inspections are specific to different types of each element, e.g., steel tunnel liner vs cast-in-place concrete tunnel liner, and the inspection outcomes are reported in terms of how much of that element falls into specified condition ranking categories. Parsing this tunnel inventory allows for determination of statistics for tunnel characteristics important to informing safety analyses. Safety analyses can be formulated using characteristics determined to be prevalent or most relevant to prioritized tunnels, where prioritization may stem from attributes such as high daily traffic loads.

## 3.0 RESULTS

The following section reports on initial parsing of tunnel characteristics from the U.S. DOT's database as well as demonstration of how lower-order modeling can be utilized explore the impact of scenario parameters on safety hazards.

### 3.1 Databased Tunnel Characteristics

Initial exploration of the National Tunnel Inventory [8] found data on many tunnel characteristics that inform the tunnel safety analysis framework on the range of specifications that should be considered. Figure 3 demonstrates three tunnel characteristics parsed from the database: minimum vertical clearance within the tunnel, tunnel length, and tunnel shape.

Annual data of tunnels in use during 2022 is shown for these three characteristics as well as a subset of the 2022 data that represents the tunnels in the top 20% of daily traffic. This data subset of high use tunnels is representative of the tunnels where tunnel safety will be of highest priority. Compared to the general population of tunnels in the U.S., the busiest tunnels are more likely to have rectangular construction and less variability in vertical clearance, while having a tunnel length distribution similar to the general population. Beyond data that can be directly parsed from the database, other information like tunnel cross sectional area and total volume can be estimated from that data.

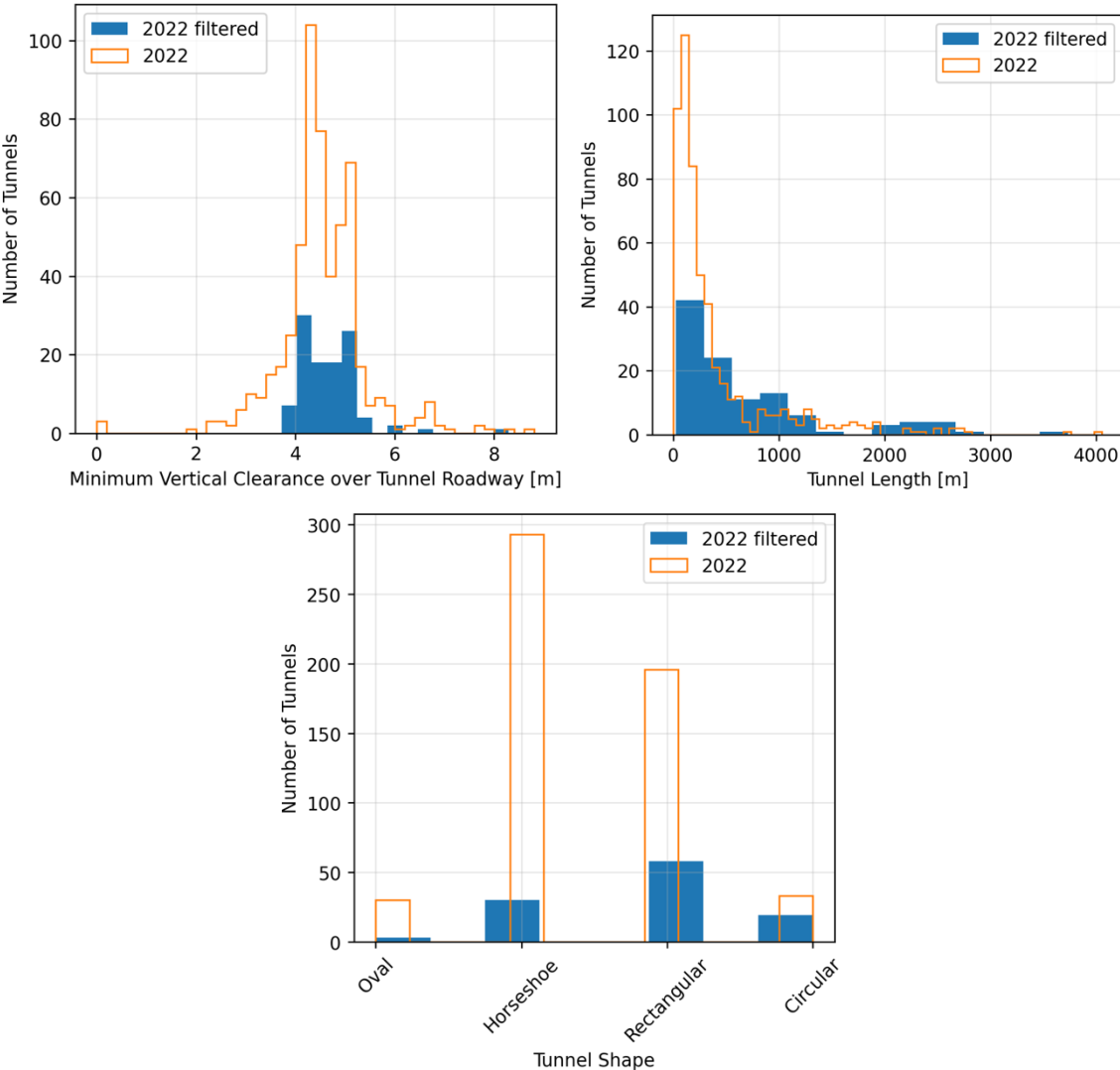


Figure 3. Tunnel characteristics parsed from U.S. tunnel inventory. 2022 filtered data only includes the top 20% of tunnels in terms of daily traffic.

### 3.2 Blowdown Predictions

Figure 4 shows the simulated blowdown of the H<sub>2</sub> tank for the overturned vehicle accident scenario. The mass flow rate, mass remaining in the fuel tank, and fuel pressure all decrease quickly, and the blowdown is completed within 5 minutes. While the duration of the blowdown is near five minutes (4.85 minutes), 75% of the mass is released from the tank in the first minute and 95% within the first three minutes. The initial flame length is predicted to be 6.9 meters long, but it quickly reduces as the mass flow rate reduces, causing the flame to no longer impinge on the ceiling after 25 seconds. The ceiling height is based on the specified distance between the release and the ceiling for the accident scenario, 3.93 meters. The flame tip temperature remains fairly constant around 2100 K while the flame is burning; the dip starting around 3.5 minutes is when the flow becomes unchoked. Radiative heat flux from the flame to the ceiling cannot be accurately predicted while the flame is impinging on the ceiling and quickly reduces as the flame blows down. Flammable mass also quickly decreases as the rate of release decreases, with the flammable mass decreasing 95% within the first 50 seconds. Initially, the overpressure 1 meter from the overpressure origin is above 21 kPa, and then decreases to 14 kPa within 50 seconds and 7 kPa within 106 seconds. As previously mentioned, the overpressure metric levels are used to estimate different levels of damage to buildings: extreme, major, and medium, respectively.

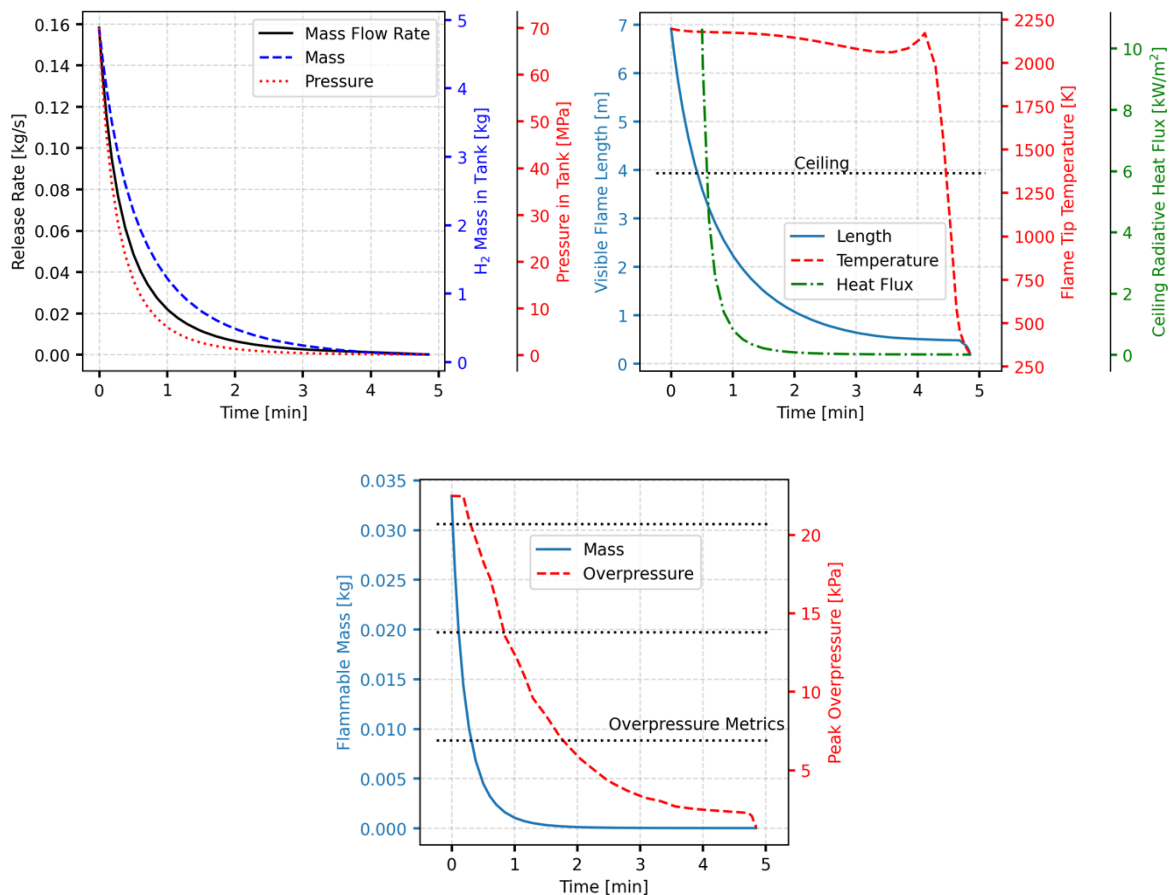


Figure 4. Blowdown characterization of H<sub>2</sub> vehicle (top left), and potential corresponding jet flame characterization (top right) and overpressure characterization (bottom)

### 3.3 Parameter Sensitivity Study

To assess the relative sensitivity of the blowdown predictions to scenario assumptions, assumptions are varied in a sensitivity study. Sensitivity cases considered include lowering the tank pressure to 35 MPa, doubling the orifice diameter, doubling the tank volume, and doubling both the orifice diameter

and the tank volume. Lowering the tank pressure represents the possibility of a partially filled tank. An increased orifice size could be due to a different TPRD design. Larger tank volumes may be representative of the sizes used in medium or heavy-duty vehicles. Figure 5 shows the blowdown results for this sensitivity study in terms of the visible flame length and the flammable mass.

Increasing the orifice size allows for a  $\sim 4x$  higher release rate, which results in  $2x$  longer flames and  $\sim 8.5x$  larger flammable masses, but also reduces the duration by over 3.5 minutes. Reducing the pressure results in 25% shorter flames and a 25% reduction in flammable mass as well as a 40 second shorter duration due to less total mass in the tank. Increasing the tank size does not impact the magnitude of the consequences but does double the duration. Increasing both the volume and orifice diameter combines the effects seen when varied separately: the same longer flame and larger flammable mass found in the calculation with only the larger orifice, but the duration is roughly twice that found for the orifice-only calculation.

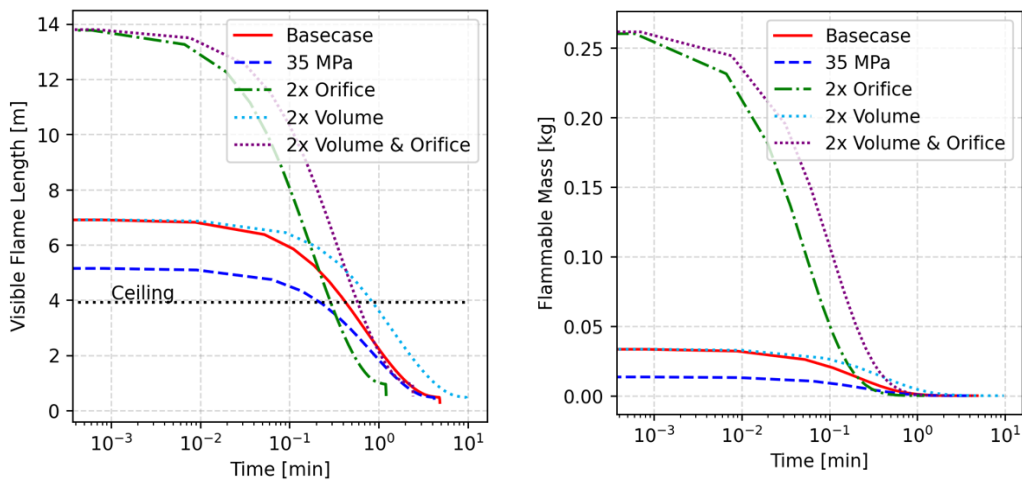


Figure 5. Assessing sensitivity of visible flame length (left) and flammable mass (right) to scenario parameters including fuel pressure, tank orifice diameter, and tank volume. Note time is shown on a log scale and that the end of the blowdowns is more clearly visible on the visible flame length plot.

### 3.4 Tank Size Study

To provide insight into how different vehicle classes could change the blowdown behaviour, a tank volume study was undertaken. Tank volumes ranged from 125 L ( $\sim 5$  kg of  $H_2$ ) up to 2,500 L ( $\sim 98$  kg of  $H_2$ ), which are meant to represent vehicle classes ranging from light duty to heavy duty, respectively. It should be noted that currently many (but not all) medium and heavy-duty vehicles have tanks that operate at 35 MPa rather than 70 MPa, so some of the effects shown here may be over-estimates in those cases. Figure 6 shows the visible flame length and flammable mass temporal profiles resulting from the blowdowns of the different tank volumes.



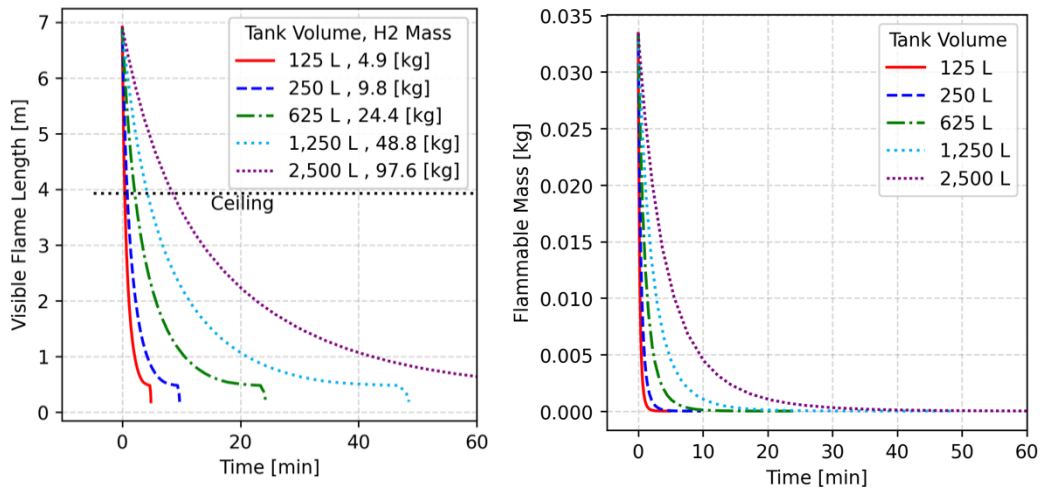


Figure 6. Assessing impact of H<sub>2</sub> tank volume on visible flame length (left) and flammable mass (right) in a blowdown scenario

As previously noted in the initial parameter study because the flow is choked for most of the release, increasing tank volume does not impact the maximum visible flame length or flammable mass, only the duration of the events, which can also be impactful in terms of the length at which the tunnel ceiling is potentially exposed to hazards. Increasing the volume to 250 L, 625 L, and 2,500 L increases the total blowdown duration 2x, 5x, and 20x, respectively. This same time scaling applies to the time for which the flame impinges on the ceiling.

### 3.5 Orifice Size Study

To assess how different TPRD sizes impact the potential consequences during blowdown, leak orifice diameters ranging from 0.5 mm up to 10 mm are simulated. These orifice sizes could be due to different TPRD designs but could also represent other types of leaks that could result from a vehicle. Figure 7 shows how the orifice diameter impacts the visible flame length and flammable mass temporal blowdown profiles.

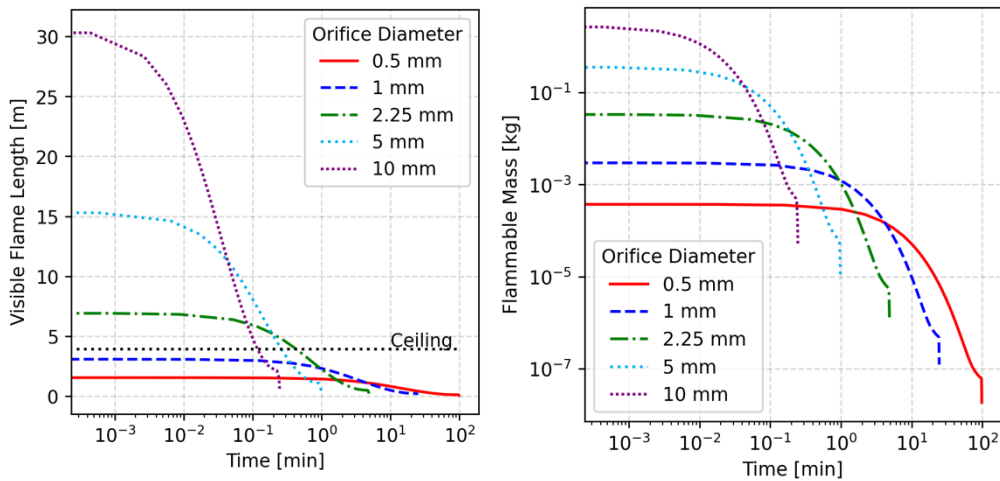


Figure 7. Assessing impact of tank orifice diameter on visible flame length and flammable mass in a blowdown scenario

Larger orifice diameters result in longer flames and larger flammable mass quantities, but for shorter durations. The 10 mm diameter orifice case has flame lengths over 30 meters long and 2.78 kg of flammable mass initially but lasted less than 15 seconds. Conversely, the flame in the 0.5 mm orifice

case never reaches the tunnel ceiling (maximum length of 1.54 m), has a maximum flammable mass less than 0.4 g, and lasts 98 minutes. Note that the dips in flammable mass occur as the flow stops being choked and may be a numerical artifact.

### 3.6 Alternative Fuels Study

To compare light duty vehicles using different types of alternative fuels, representative tank configurations are estimated. Figure 8 shows a comparison of a fuel tank blowdown of H<sub>2</sub>, CNG (CH<sub>4</sub>), and LPG vehicle fuel tanks in terms of the potential resulting flame length and flammable mass.

The fuel mass for each fuel tank is shown in the legend of the visible flame length plot (left). Even though the H<sub>2</sub> tank is at the highest pressure, due to its low volumetric energy density it has less mass than the CNG tank. Given its liquid form, the LPG fuel tank contains the largest fuel mass. While clearly this comparison is not on an equal mass basis, it represents fieldable tanks for each fuel type. The CNG and H<sub>2</sub> flames both significantly surpass the ceiling height, while the LPG flame also reaches the ceiling, but with much less margin. The H<sub>2</sub> and CNG tanks also have significantly higher flammable masses than the LPG tank, with the initial H<sub>2</sub> flammable mass being more than double the CNG result. Comparing the gaseous fuels to the liquid fuel, the responses for gaseous fuels have convex curvature compared to the concave curvature of the responses for liquid fuels. This curvature difference is due transition of the liquid fuel to gas prior to release from the tank. The LPG tank’s most notable characteristic is its long release time (over 22 minutes) compared to the under 5 minutes of H<sub>2</sub> and under 8 minutes for CNG.

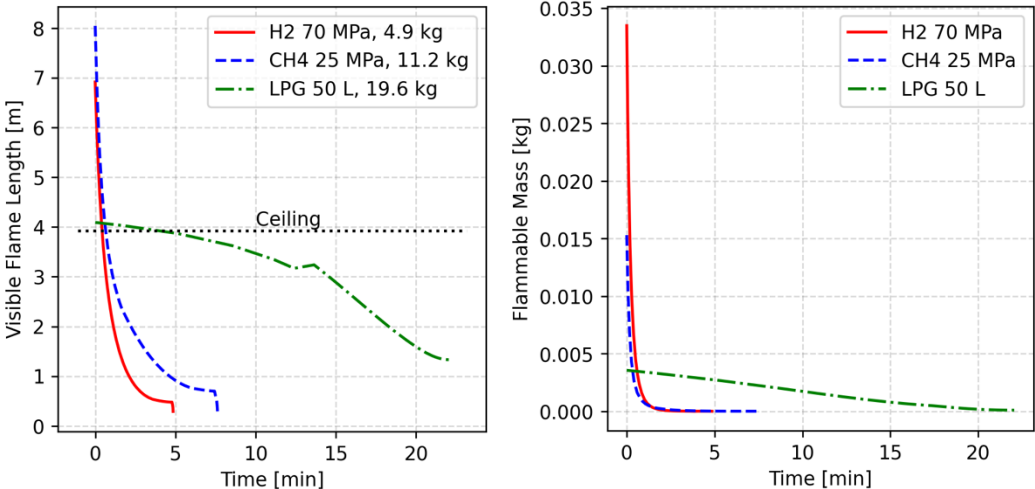


Figure 8. Comparing alternative fuelled vehicles in terms of visible flame length (left) and flammable mass (right) in a blowdown scenario

### 3.7 Tank Fullness Study

It has been previously assumed that the crashed H<sub>2</sub> vehicle has a full tank of fuel at the time of the incident. In terms of consequences this is a worst-case scenario. To assess the impact of this assumption, blowdown calculations are performed for tanks with different levels of fullness on a mass basis ranging from full to 1/8 full. Figure 9 shows the flame length and overpressure events that could result from tank blowdowns for the different tank fill levels.

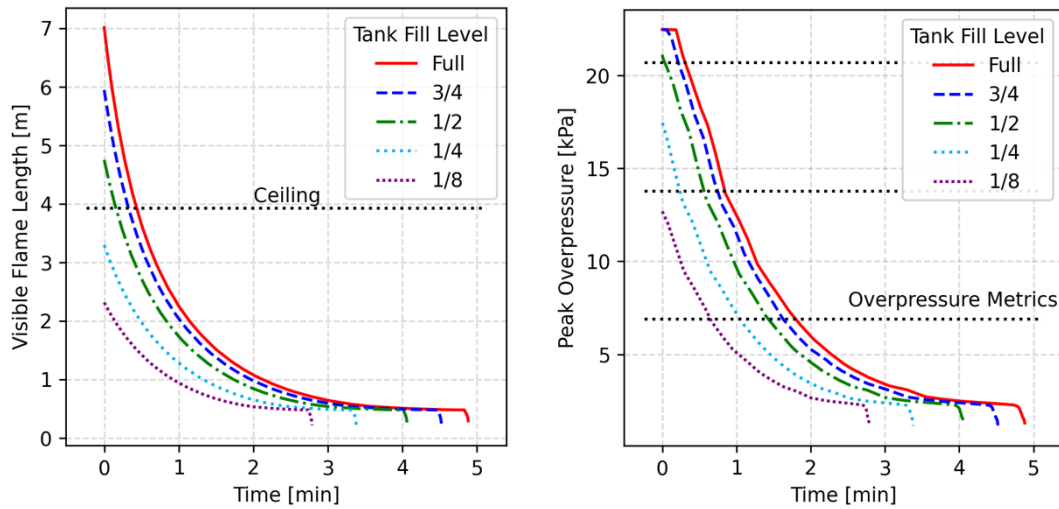


Figure 9. Assessing impact of tank fullness on potential visible flame length (left) and peak overpressure (right) in a blowdown scenario

Once the tank is between  $\frac{1}{2}$  and  $\frac{1}{4}$  full, the potential flame no longer reaches the ceiling and the maximum overpressure 1 meter away from the overpressure event origin is below the 20.7 kPa damage metric. The level of tank fill impacts both the magnitude of potential consequences, as well as the duration.

### 3.8 Fuel Dispersion Volume Study

As part of the effort to investigate the possibility of developing large flammable masses of fuel within tunnels, a physically impossible extreme case was computed. For this case the total volume of  $H_2$  at its lower flammability limit is computed for the range of  $H_2$  masses previously investigated in the tank size study, which was meant as an estimate for different vehicle classes. A lower flammability limit of 4% by volume was used for this study. It should be noted that this is an overly simplistic consideration of flammable volumes; hydrogen will continue to dissipate and dilute even as the leak continues to release more hydrogen. It is impossible to have a physical scenario in which the entire inventory of hydrogen contributes to flammable mass with none of it being diluted to below the flammable limit but it is examined here to cover the most conservative scenario. Figure 10 shows how the volume of  $H_2$  mixed with air at  $H_2$ 's lower flammability limit scales with the total mass of  $H_2$  stored in a fuel tank and compares those volumes to estimated volumes for tunnels.

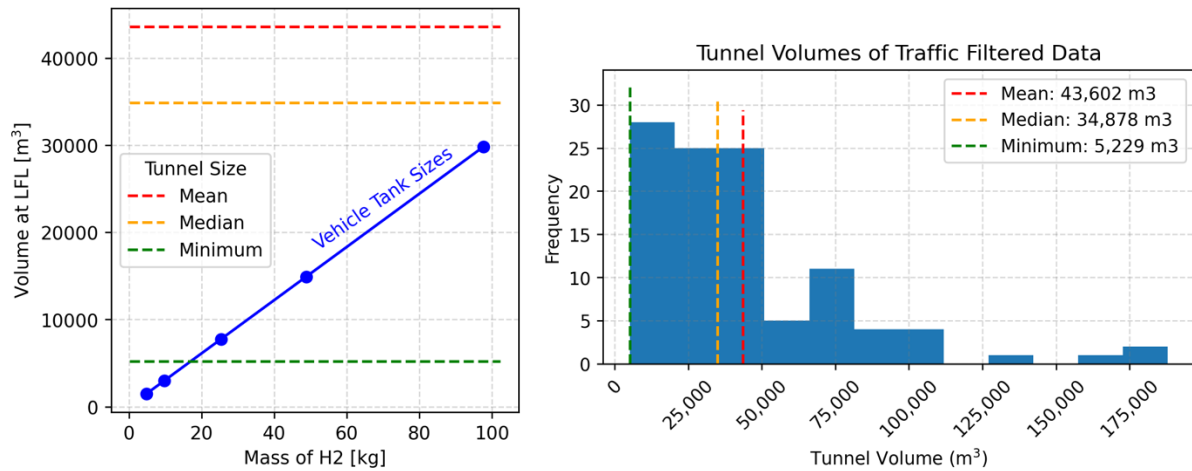


Figure 10. Comparing total volume of H<sub>2</sub> if diluted down to lower flammability limit for different masses of stored H<sub>2</sub> (left) with tunnel volumes for top 20% of tunnels in terms of daily traffic (right)

Tunnel volumes were estimated based on National Tunnel Inventory data on tunnel shape, vertical clearance, roadway width, sidewalk width, and length. The tunnels whose volume is used for the comparison are the top 20% of U.S. tunnels in terms of daily traffic. Light duty vehicles (carrying around 5 or 10 kgs of H<sub>2</sub>) could fill up volumes (1,500 or 3,000 m<sup>3</sup>) smaller than the smallest tunnel considered (5,229 m<sup>3</sup>). Only the heavy-duty vehicles carrying nearly 100 kg of H<sub>2</sub> (29,800 m<sup>3</sup>) approach the median tunnel size (34,878 m<sup>3</sup>). While the many assumptions used in this study make the predictions unrealistic (ignoring buoyancy and ventilation), it provides a means of visualizing the relative size of flammable mass volumes potentially produced in accidents compared to tunnel volumes.

#### 4.0 CONCLUSIONS

The presented work represents first steps towards developing a generalized tunnel safety analysis, focusing on alternative vehicles. Representative ranges of tunnel characteristics are accessible from the U.S. DOT's National Tunnel Inventory comprised of over 550 tunnels. Lower-order consequence models enable efficient exploration of wide ranges of crash scenario parameters. By varying scenario parameters, insights into the impact on resulting hazards can be quickly quantified. Calculations using lower-order consequence models within HyRAM+ provided temporally evolving estimates of hazards potentially impacting the structure integrity of tunnel ceilings including the ceiling gas temperature and nearby overpressure events. Scenario parameters studied within this work included the tank volume, representative of different vehicles classes; the orifice diameter, representative of different TPRDs; the tank fill level, representative of the reality that fuel tanks are often only partially filled during operation; and the fuel type, providing comparisons between alternative fuel types. While ventilation effects were not considered, scenarios without ventilation tend to produce more harmful consequences, so the cases studied here represent a worst-case scenario. Integration of the lower-order consequence models with data-based tunnel characteristics is an example of how a generalized tunnel safety analysis framework could be utilized to quickly provide safety sights to tunnel owners.

Future steps in the development of a generalized tunnel safety analysis framework will include integration of additional analysis elements. Information from tunnel design codes and standards [9] as well as material response characterization need to be connected to the consequence modeling to enable assessment of tunnel structural response. Analysis of heat transfer to common tunnel construction materials will help determine whether the temperatures reached will cause significant damage. Baseline comparisons with the high-fidelity modeling can be undertaken and used to understand the predictive performance of the lower-order calculations. Including the impact of ventilation systems on the lower-fidelity modeling would allow for the accounting of an additional, commonly used safety

feature. Integration of these analysis elements will ultimately comprise the envisioned generalized tunnel safety analysis framework.

## ACKNOWLEDGEMENTS

This work was supported by the Department of Energy Office of Energy Efficiency and Renewable Energy Hydrogen and Fuel Cell Technologies Office, as part of the Safety Codes and Standards program under the direction of Laura Hill. This article has been authored by an employee of National Technology & Engineering Solutions of Sandia, LLC under Contract No. DE-NA0003525 with the U.S. Department of Energy (DOE). The employee owns all right, title and interest in and to the article and is solely responsible for its contents. The United States Government retains and the publisher, by accepting the article for publication, acknowledges that the United States Government retains a non-exclusive, paid-up, irrevocable, world-wide license to publish or reproduce the published form of this article or allow others to do so, for United States Government purposes. The DOE will provide public access to these results of federally sponsored research in accordance with the DOE Public Access Plan <https://www.energy.gov/downloads/doe-public-access-plan>. This paper describes objective technical results and analysis. Any subjective views or opinions that might be expressed in the paper do not necessarily represent the views of the U.S. Department of Energy or the United States Government.

## REFERENCES

1. LaFleur, C., Muna, A.B., Ehrhart, B.D., Bran-Anleu, G.B., Blaylock, M., and Houf, W.G., Hydrogen Fuel Cell Electric Vehicle Tunnel Safety Study, Sandia National Laboratories Report No. SAND2017-11157, Oct. 2017.
2. LaFleur, C.B., Glover, A.M., Baird, A.R., Jordan, C.R., Ehrhart, B.D., Alternative Fuel Vehicles in Tunnels, Sandia National Laboratories Report No. SANS2020-5466, May 2020.
3. Saw, J.L, Rattigan, W., Moodie, K, Bergin, S., Cirrone, D. Molkov, V., and contributing authors, Deliverable D6.9: Recommendations for inherently safety use of hydrogen vehicle in underground traffic systems, HyTunnel project, Clean Hydrogen Joint Undertaking (FCH JU), 2022.
4. <https://response.restoratoin.noaa.gov/oil-and-chemical-spills/resources/overpressure-levels-concerns.html>, Accessed Feb. 2023
5. <https://energy.sandia.gov/programs/sustainable-transportation/hydrogen/hydrogen-safety-codes-and-standards/hyram/>, Accessed Feb. 2023.
6. Ehrhart, B.D. and Hecht, E.S., Hydrogen Plus Other Alternative Fuels Risk Assessment Models (HyRAM+) Version 5.0 Technical Reference Manual, Sandia National Laboratories Report No. SAND2022-16425, Nov. 2022.
7. Guo, Q., Hecht, E.S., Blaylock, M.L., Shum, J.G., and Jordan, C., Physics model validation of propane and methane for Hydrogen Plus Other Alternative Fuels Risk Assessment Models (HyRAM+), *Process Safety and Environment Projection*, **173**, 2023, pp. 22-38.
8. <https://www.fhwa.dot.gov/bridge/inspection/tunnel/inventory.cfm>, Accessed Nov. 2022
9. NFPA 502, Standard for Road Tunnels, Bridges, and Other Limited Access Highways, 2017.